Measurement of ϕ_s in Run2 at LHCb

P. Muzzetto on behalf of the LHCb Collaboration

Università di Cagliari - Cagliari, Italy

received 8 June 2020

Summary. — Two recent measurements of CP-violating parameters are presented, obtained using proton-proton collision data collected by the LHCb detector in 2015 and 2016 at a centre-of-mass energy of 13 TeV. In particular, the measurement of the CP-violating phase ϕ_s using a time-dependent analysis of the $B_s \to J/\psi K^+ K^-$ and $B_s \to J/\psi \pi^+ \pi^-$ channels is described.

1. – Introduction

The Standard Model (SM) very successfully describes experimental observations, but fails to explain, among others, the amount of matter-antimatter asymmetry observed in the Universe. New physics phenomena not described by the SM, as new particles contribution to the B_s^0-meson mixing diagrams, could substantially modify the magnitude of Charge-Parity (CP) violating parameters. Thanks to its very precise determination in the SM, one of the most sensitive observables is the CP-violating phase ϕ_s, that arises from the interference between B_s^0 meson decay amplitudes via $b \to c\bar{c}s$ direct transition or via mixing. Ignoring subleading penguin contributions, its SM value determined via global fits to experimental data is -0.0364 ± 0.0016 rad [1]. Here, the most recent measurements of the CP-violating phase ϕ_s, obtained exploiting the data collected by the LHCb detector and using a time-dependent analysis of the $B_s \to J/\psi K^+ K^-$ and $B_s \to J/\psi \pi^+ \pi^-$ decay channels, are reported. The LHCb detector [2,3] is a single-arm forward spectrometer covering the pseudorapidity range $2 < \eta < 5$, designed for the study of particles containing b or c quarks.

2. – Measurement of ϕ_s at LHCb

The decay mode $B_s^0 \to J/\psi K^+ K^-$ is the golden channel to measure ϕ_s, due to its high statistics and clean experimental signature thanks to the two muons in the final state, followed by the $B_s^0 \to J/\psi \pi^+ \pi^-$ decay. For both channels, the decay proceeds

predominantly via a tree-level $b \rightarrow c\bar{c}s$ transition. This allows to neglect the sub-leading higher-order contributions and to compare the measurement with the very precise prediction of the SM. Both analyses use proton-proton collision data collected by the LHCb experiment in 2015 and 2016, corresponding to a total integrated luminosity of $1.9\,\text{fb}^{-1}$. Since ϕ_s is related to the magnitude of the $B_s^0 - \bar{B}_s^0$ oscillations, two time-dependent analyses have been performed and, since the decay rate depends on the CP eigenvalue of the final state, an angular analysis is carried out too. This allows to measure simultaneously the mixing and lifetime parameters of the B_s^0 meson. For both analyses the helicity angles basis [4] is used, describing the four-body final states with three angles.

For an initial B_s^0 the experimental differential decay rate as a function of decay-time and angles [5], taking into account different detector and analysis effects, is

$$(1) \qquad \frac{\text{d}^4\Gamma(t)}{\text{d}\Omega\text{d}t} = \sum_{k=1}^{10} \epsilon(t,\Omega) f_k(\Omega) h_k(t) \otimes G(t|\sigma_t),$$

where $\epsilon(t,\Omega)$ is the angular and decay-time efficiency, $G(t|\sigma_t)$ is the decay-time resolution, $f_k(\Omega)$ are angular functions and $h_k(t)$ are the decay-time-dependent functions given by

$$(2) \qquad h_k(t) = \frac{3}{4\pi} e^{-\Gamma t} \left\{ a_k \cosh\frac{\Delta\Gamma t}{2} + b_k \sinh\frac{\Delta\Gamma t}{2} + c_k \cos(\Delta m t) + d_k \sin(\Delta m t) \right\}.$$

For an initial $\bar{B}_s^0$ at production, the signs of c_k and d_k should be reversed. A simultaneous maximum likelihood fit of the decay-time and the three angles is performed and, depending on the decay mode, different parameters are measured in addition to ϕ_s and $|\lambda|$. The analysis on $B_s^0 \rightarrow J/\psi K^+ K^-$ [6] is developed requiring the invariant mass of the $K^+ K^-$ system being in a window around the $\phi(1020)$ resonance. Since the $B_s^0 \rightarrow J/\psi K^+ K^-$ final state is not a pure CP-eigenstate, the decay-width difference between the light (L) and heavy (H) B_s^0 meson eigenstates $\Delta\Gamma_s = \Gamma_L - \Gamma_H$ and its average decay width $\Gamma_s = \frac{\Gamma_H + \Gamma_L}{2}$ are measured. In the $B_s^0 \rightarrow J/\psi \pi^+ \pi^-$ analysis [7] only the measurement of Γ_H is possible, because the final state is almost entirely CP-odd.

2'1. Selection strategy and mass fit. – The suppression of the combinatorial background is performed using an optimised boosted decision tree, (BDT) [8], for both channels. The BDTs are trained using simulated samples to describe the signal and data sidebands as a proxy for the background. Before the BDTs training, both simulated samples have been corrected to match pure signal data samples. Different types of misidentified backgrounds are also taken into account in the selection procedure. The peaking background contributions coming from $B^0 \rightarrow J/\psi K^{*0}(\rightarrow K^+\pi^-)$ for both channels and $B^+ \rightarrow J/\psi K^+$ for $B_s \rightarrow J/\psi \pi^+ \pi^-$ decay are vetoed requiring particle identification selections, while the contributions from $B \rightarrow J/\psi K^+ K^-$ and $B \rightarrow J/\psi \pi^+ \pi^-$ are directly accounted in the mass fits. The $\Lambda_b \rightarrow J/\psi p^+ K^-$ background is treated differently, because it populates the signal region and cannot be completely suppressed by particle identification requirements. The strategy, common to the two analyses, is to subtract it by injecting an amount of negatively weighted simulated events of $\Lambda_b \rightarrow J/\psi p^+ K^-$ decays, equal to the expected contribution to the data samples. The same method is used for the $B_s \rightarrow J/\psi \pi^+ \pi^-$ decay channel in order to reject the misidentified contribution of $B_s^0 \rightarrow J/\psi \eta'(\rightarrow \rho\gamma)$ decays and the combinatorial background contribution, where the
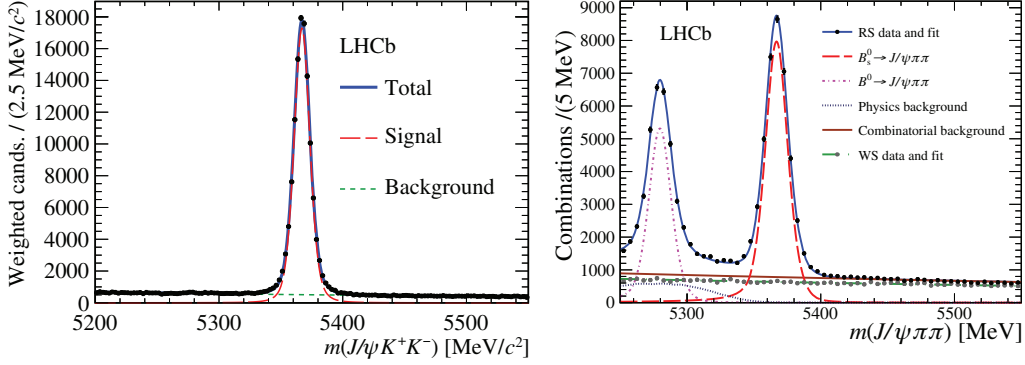
Fig. 1. – Distribution of the invariant mass of selected $B_s \rightarrow J/\psi K^+ K^-$ (left) and $B_s \rightarrow J/\psi \pi^+ \pi^-$ (right) events with overlayed result of an unbinned maximum likelihood fit.

individual amount of events is directly determined in the mass fit, shown in fig. 1(right). In order to statistically subtract the combinatorial background for the $B_s \rightarrow J/\psi K^+ K^-$ decay channel, the sPlot [9] technique is used. This procedure assigns an event-by-event weight based on the probability density function used to describe the B_s^0 invariant mass spectra. The sum of weights is equal to the number of signal events extrapolated by the fit of the mass distribution, shown in fig. 1(left).

2‘2. *Decay-time resolution.* – Since ϕ_s is closely related to the oscillation amplitude of the $B_s^0 - \bar{B}_s^0$ system, a detailed knowledge of the decay-time resolution is fundamental. A first estimation of the event-by-event time resolution is obtained calculating the decay-time uncertainty δt during the reconstruction procedure, but it tends to be underestimated, thus a calibration is required. For this purpose, a sample of real J/ψ's coming from the interaction point plus two opposite-sign charged tracks, so-called prompt sample, is used. Since this sample has by construction a lifetime equal to zero, the width of the decay-time distribution is due to the time resolution effect of the detector only. Using this sample, the decay-time distribution is studied in bins of δt. A fit with a triple-Gaussian model is performed and an effective single-Gaussian time resolution for each bin is obtained. The decay-time resolution variation as a function of δt is modelled with a quadratic function. Relative results for $B_s^0 \rightarrow J/\psi K^+ K^-$ decay mode are shown in fig. 2. For $B_s \rightarrow J/\psi K^+ K^-$ the effective resolution turns out to be about 45.5 fs, while for $B_s \rightarrow J/\psi \pi^+ \pi^-$ the value is 41.5 fs.

2‘3. *Angular and time efficiency.* – Because of detector and selection effects, the angular and decay-time distributions are affected by a non-uniform efficiency. For both the analyses, the decay-time efficiency is mainly due to displacements requirements implemented in the trigger selection. In order to correct for this effect, the control channel $B^0 \rightarrow J/\psi K^*(892)^0$ is used, which has a well-known lifetime $\tau_{B^0} = 1.520 \pm 0.004$ ps [10] and a kinematics very similar to the channels under study. The time efficiency is extracted using a data-driven method as

$$(3) \qquad \epsilon_{data}^{B_s^0}(t) = \epsilon_{data}^{B^0}(t) \times \frac{\epsilon_{sim}^{B_s^0}(t)}{\epsilon_{sim}^{B^0}(t)},$$
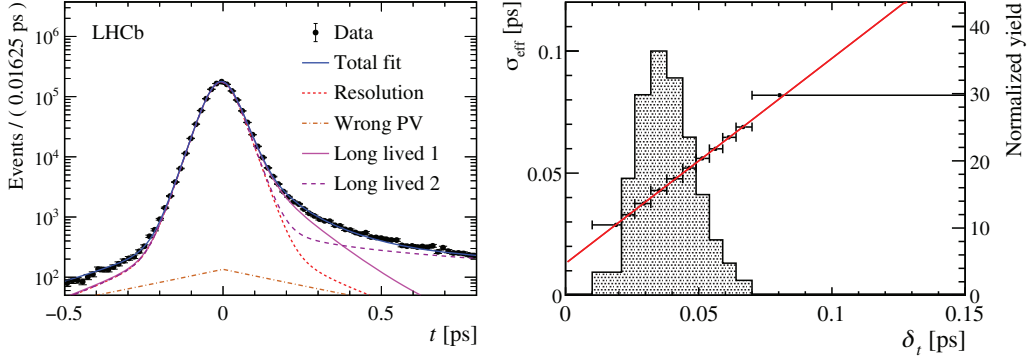
Fig. 2. – Left: decay-time distribution of the prompt $J/\psi K^+ K^-$ calibration sample with the result of an unbinned maximum-likelihood fit overlaid in blue. Right: variation of the effective single-Gaussian decay-time resolution as a function of the estimated per-candidate decay-time uncertainty, δt. The red line shows the result of a linear fit. The data points are positioned at the barycentre of each δt bin. The shaded histogram (see right y-axis) shows the distribution of δt in the background-subtracted $B_s^0 \to J/\psi K^+ K^-$ sample.

where each efficiency is described with a cubic spline and a small correction taken from simulated data is used to take into account differences between signal and calibration samples. For both decay modes, the angular efficiencies are instead fully evaluated using simulated signal events. For $B_s^0 \to J/\psi \pi^+ \pi^-$ decay mode, an additional efficiency as a function of the invariant mass spectra of the two pions, $m(\pi\pi)$, is also studied. The efficiencies effects are taken into account in the final fit according to eq. (1).

2·4. *Flavour tagging.* – The decay-time-dependent functions given in eq. (2), change with the B_s^0 flavour at production. Therefore, a detailed understanding of the B_s^0 flavour is required. For both decay channels two different algorithms are used to infer the
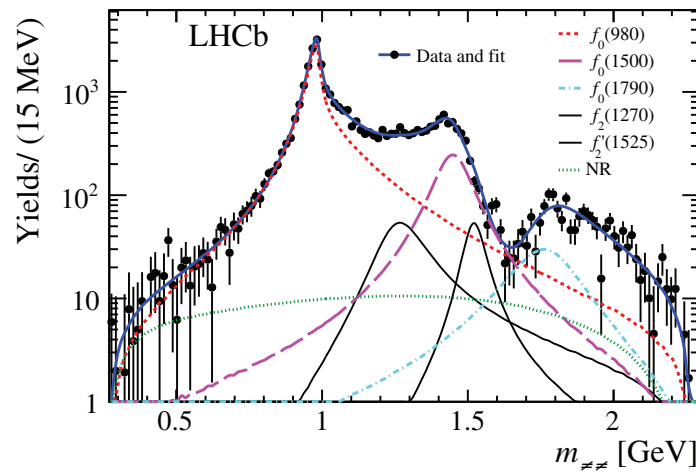

Fig. 3. – Data distribution of $m(\pi\pi)$ with the projection of the fit result overlaid.

TABLE I. – *Data fit results for the CP-violating parameters measured using $B_s^0 \to J/\psi K^+ K^-$ and $B_s^0 \to J/\psi \pi^+ \pi^-$ decay modes. The first uncertainties are statistical, and the second when quoted are systematic. If only one is given then it is a combination of both statistical and systematic uncertainties calculated under the assumption that those contributions are independent. In the last column the results combined with all the previous measurements of the ϕ_s phase performed by the LHCb experiment are shown.*

Observable	$B_s^0 \to J/\psi K^+ K^-$	$B_s^0 \to J/\psi \pi^+ \pi^-$	Combined values
ϕ_s (rad)	$-0.080 \pm 0.041 \pm 0.006$	$-0.057 \pm 0.060 \pm 0.011$	-0.040 ± 0.025
$|\lambda|$	$1.006 \pm 0.016 \pm 0.006$	$1.01^{+0.08}_{-0.06} \pm 0.03$	0.991 ± 0.010
$\Gamma_{s/H} - \Gamma_d$ (ps^{-1})	$-0.0041 \pm 0.0024 \pm 0.0015$	$-0.050 \pm 0.04 \pm 0.004$	-0.0024 ± 0.0018
$\Delta\Gamma_s$ (ps^{-1})	$0.0772 \pm 0.0077 \pm 0.0026$	–	0.0813 ± 0.0048

flavour. The Same Side (SS) tagger exploits the particle (kaon) produced during the fragmentation process of the signal B_s^0, while the Opposite Side (OS) tagger uses the decay products of the other b hadron produced in the event. The tagging performance is not perfect, because a wrong track can be selected to tag the event and, in the case of
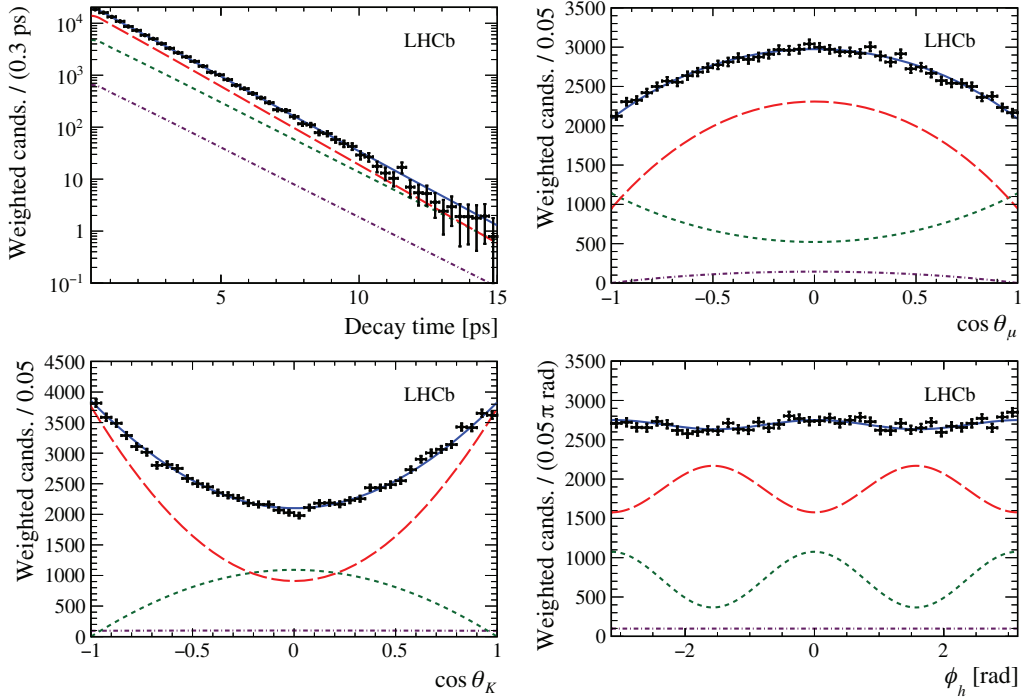

Fig. 4. – Decay-time and helicity-angle distributions for background-subtracted $B_s^0 \to J/\psi K^+ K^-$ decays (data points) with the one-dimensional projections of the PDF at the maximum-likelihood point. The solid blue line shows the total signal contribution, which contains (long-dashed red) CP-even, (short-dashed green) CP-odd and (dot-dashed purple) S-wave contributions.
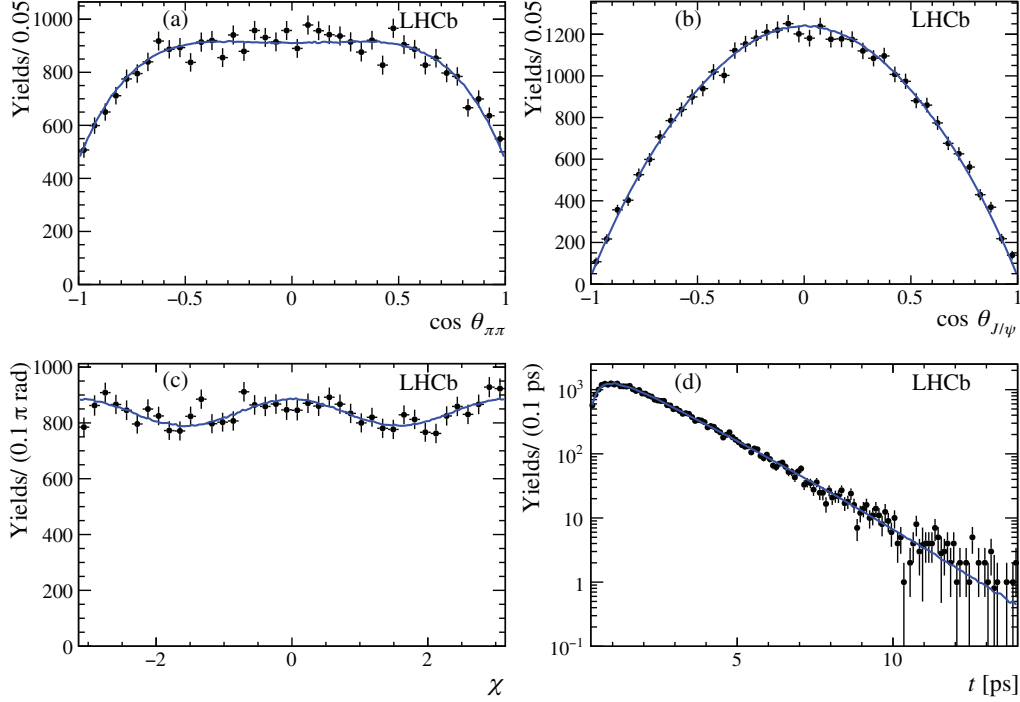
Fig. 5. – Decay-time and helicity-angle distributions for background-subtracted $B_s^0 \to J/\psi\pi^+\pi^-$ decays (data points) with the one-dimensional projections of the PDF at the maximum-likelihood point. The solid blue line shows the total signal contribution.

OS tagger, a possible neutral opposite B can oscillate, producing an intrinsic dilution. Therefore, the taggers have to be calibrated using flavour-specific decay channels, in particular a data sample of $B^+ \to J/\psi K^+$ decays for the OS tagger and a data sample of $B_s^0 \to D_s^- \pi^+$ for the SS tagger. Finally the results of the two taggers are combined to obtain a better identification power, equal to $4.73 \pm 0.34\%$ for $B_s \to J/\psi K^+ K^-$ channel and $5.06 \pm 0.38\%$ for $B_s^0 \to J/\psi\pi^+\pi^-$ decay.

3. – Results

For both analyses, an angular and time-dependent unbinned maximum likelihood fit on the experimental decay-time distribution and helicity angles is performed, using $1.9\,\text{fb}^{-1}$ of proton-proton collision data collected by the LHCb experiment during 2015 and 2016. For the $B_s^0 \to J/\psi\pi^+\pi^-$ decay mode an amplitude analysis in the mass of two pions is also carried out and the corresponding distribution with fit projections is shown in fig. 3. The results are shown in table I. The analysis of $B_s^0 \to J/\psi K^+ K^-$ provides the most precise measurement of CP violation parameters arising from the interference of B_s^0 mixing and decay to date. This result, combined with those from $B_s^0 \to J/\psi\pi^+\pi^-$ decays and with previous independent ones performed by LHCb [11-14], are compatible with the SM expectations and with no CPV in the decay modes. The background-subtracted projection plots are shown for $B_s^0 \to J/\psi K^+ K^-$ decay in fig. 4 and for $B_s^0 \to J/\psi\pi^+\pi^-$ in fig. 5.

REFERENCES

[1] CHARLES J. *et al.*, *Phys. Rev. D*, **84** (2011) 033005.
[2] LHCb COLLABORATION (ALVES A. A. jr. *et al.*), *JINST*, **3** (2008) S08005.
[3] LHCb COLLABORATION (ALVES A. A. jr. *et al.*), *Int. J. Mod. Phys. A*, **07** (2015) 1530022.
[4] LHCb COLLABORATION (ALVES A. A. jr. *et al.*), *Phys. Rev. D*, **87** (2013) 112010.
[5] LIU XIN, WANG WEI and XIE YUEHONG, *Phys. Rev. D*, **89** (2014) 094010.
[6] LHCb COLLABORATION (AAIJ R. *et al.*, *Eur. Phys. J. C*, **79** (2019) 706.
[7] LHCb COLLABORATION (AAIJ R. *et al.*), *Phys. Lett. B*, **797** (2019) 134789.
[8] BREIMAN L., FRIEDMAN J. H., OLSHEN R. A. and STONE C. J., *Classification and Regression Trees* (Wadsworth International Group, Belmont) 1984.
[9] PIVK M. and LE DIBERDER F. R., *Nucl. Instrum. Methods A*, **555** (2005) 356.
[10] PARTICLE DATA GROUP (TANABASHI M. *et al.*), *Phys. Rev. D*, **98** (2018) 030001.
[11] LHCb COLLABORATION (AAIJ R. *et al.*), *Phys. Lett. B*, **736** (2014) 186.
[12] AAIJ R. *et al.*, *Phys. Lett. B*, **762** (2016) 253.
[13] LHCb COLLABORATION (AAIJ R. *et al.*), *Phys. Rev. Lett.*, **113** (2014) 211801.
[14] LHCb COLLABORATION (AAIJ R. *et al.*), *JHEP*, **08** (2017) 37.